

Integration of seismic first arrival times to estimate water-air contact and initial water saturation



Ting Sun ^{a,*}, Yuanyuan Shuai ^b, Christopher White ^c, Juan Lorenzo ^d, Shannon Chollett ^d

^a China University of Petroleum, Beijing, China

^b Shell Oil Company, Houston, TX, USA

^c Tulane University, New Orleans, LA, USA

^d Louisiana State University, Baton Rouge, LA, USA

ARTICLE INFO

Article history:

Received 20 December 2016

Received in revised form

30 April 2017

Accepted 7 May 2017

Available online 27 May 2017

Keywords:

Data integration

Seismic first arrival times

Trust region method

Water-air contact

Initial water saturation

ABSTRACT

History matched models have helped reservoir engineers obtain a better understanding of the reservoir and optimize the future productions. Recent years, seismic data is more often to be integrated to improve the reservoir models, however, seismic data has to be inverted to seismic impedance values first.

In this study, we introduce a new way to improve the initial reservoir models -integrating the seismic first arrival times to estimate the fluid contacts and initial water saturation. The key aspect of this method that distinguishes it from other methods is that seismic data is integrated directly. As a result, traditional seismic inversion step is not needed, and the data integration are through the comparison of observed first arrival times and simulated first arrival times (raytracing results).

In our paper, the feasibility of using seismic first arrival times to improve initial reservoir models is discussed, and the method is verified by using sand tank experiment data. The observed seismic first arrival times were collected during the experiment, and the simulated first arrival times were calculated by seismic raytracing program. Trust region method was used to adjust water-air contact depth and initial water saturation to minimize the difference between simulated and observed data. At last, a good estimation of initial condition is achieved, and it demonstrates a potential of integrating seismic data to improve the reservoir models without an inversion step.

© 2017 Elsevier B.V. All rights reserved.

1. Introduction

Improved modeling has helped to optimize reservoir development. To reduce the inherent uncertainty of the models and obtain more predictive simulations, more data should be integrated into the geomodels. Production data, such as bottom hole pressure, gas oil ratio and water oil ratio have been widely used in history matching. Interwell tracer tests and well testing also provide additional sources of data (Thulin et al., 2007; Li et al., 2009; Valestrand et al., 2010). However, sometime we still could not have a good estimation of reservoir properties with these data, since they can provide high resolution estimation around well locations, but the properties in regions far from wells remain poorly constrained. To reduce uncertainty in estimation, seismic data can be integrated with production data to provide denser information across whole field. Many investigators have addressed seismic data

integration and proved that seismic data can help improve the reservoir models. Dong (2005) applied the ensemble Kalman filter (EnKF) method to rapidly update the estimation of the model variables in a small synthetic case which shows that it is possible to integrate both time-lapse seismic impedance data and production data. Emerick, de Moraes, and Rodrigues (2007) integrated time-lapse seismic attributes into a derivative-based assisted history matching tool; their optimization algorithm was based on a trust-region quasi-Newton method to minimize the mismatch between observed and simulated data from production and seismic. A method based on the combination of EnKF and ensemble Kalman smoother (EnKS) (Skjervheim et al., 2007) used a combination of production data and 4D seismic data. Their method was tested on a synthetic case and a real North Sea field case. For both the synthetic and field case, a better permeability estimate was obtained by including both seismic data and production data. For the 2D synthetic problem, better estimates of the permeability were obtained by integrating inverted seismic data at the time they were measured instead of using 4D data. Zhao, Reynolds, and Li (2008) proposed integrating seismic data (acoustic impedance data) at

* Corresponding author.

E-mail address: upcxiaos@gmail.com (T. Sun).

two separate times together with production data. They gave an ensemble of facies maps closer to the “true model” and better estimates of future performance than the ones obtained from the models updated by production data only.

As noted above, the integration of seismic data is mainly focusing on the integration of time-lapse seismic data which is the differences of seismic impedances at two different times, it can be integrated to improve the reservoir models. However, the integration of time-lapse seismic data still has several drawbacks. First, it could not be integrated if there is not enough changes between two seismic impedances. Second, the time-lapse method generally assumes that the source and receiver do not change over time which is usually several years, even more than ten years. Third, seismic data first has to be inverted to seismic impedance values, which are nonunique (Saltzer and Finn, 2006). For example, using the same seismic data, many different seismic impedance datasets can be obtained, all of which are plausible.

Because of the shortcomings of time-lapse seismic data listed above, integrating seismic data directly without a separate inversion step is a promising approach. Since the seismic data contains a huge volume of data and many noises, a lot of research work needs to be done for integrating them directly. In this paper, our objective is to investigate the feasibility of integrating the seismic first arrival times to improve the initial reservoir models. In this method, seismic inversion step is not needed. The method was verified on a meter-scale experiment – sand tank experiment and we will see how the integration of first arrival times affects the predictions. The automatic optimization method used here is trust region method, since it is very efficient when there are only limited number of the variables need to adjust (less than one hundred).

The outline of this paper is described as follows. First, a brief introduction of seismic first arrival times and the trust region method; secondly, the sand tank experiment is introduced, and the feasibility of integrating seismic first arrival times is analyzed; then, the seismic first arrival times in the sand tank experiment are integrated to update the depth of water-air contact and initial water saturation using trust region method, and the results are discussed. Finally a conclusion will be given.

2. Feasibility of integrating seismic first arrival times

There are two reasons that the seismic first arrival times are feasible to be integrated: firstly, the seismic first arrival times are the first signals detected by the geophones, and because the earliest portion of the seismic record is often dominated by source generated noise, first arrival times are more accurate and can be more clearly identified than the rest of wave data; secondly, the path of seismic waves depend on the spatial variation of acoustic velocity in the vicinity of the source and geophone, and acoustic velocity could be calculated using density and elastic moduli which are influenced by both the mineral and fluid properties (Appendix A). Fig. 1 shows the relationship between velocity and saturation based on the Hertz-Mindlin method and the Biot-Gassmann theory, assuming that other parameters are constant. For low saturations, the velocity decreases as saturation increases. Above a water saturation of 96 percent, the velocity begins to increase. The velocity increases sharply when the saturation is higher than 99 percent. Based on the above conclusion, it is reasonable to attempt to integrate the seismic first arrival times to decrease flow model uncertainty.

3. Trust region method

In this paper, trust region method is used as integration method, since it works very efficiently when the number of tuning

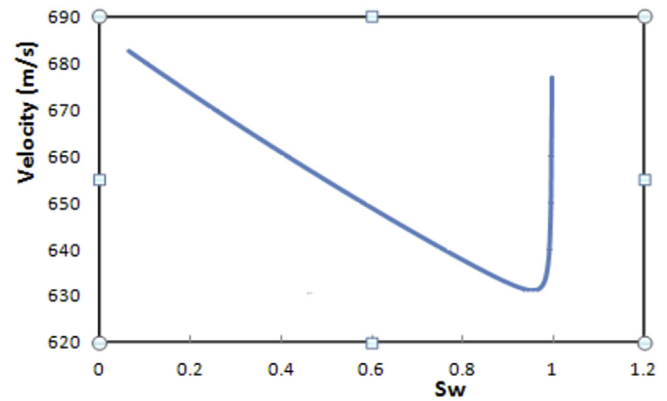


Fig. 1. Saturation versus velocity by Gassmann theory, Biot equation and Hertz-Mindlin method. The velocity is calculated when the saturation is in the range between 0.06 and 0.99, and all the other parameters, such as coordination number and porosity, are constant.

parameters is less than one hundred. Trust region method is one of the most well-known techniques in solving nonlinear programming problem (reference). It is closely related to approximation. First, it assumes a best solution of the optimization problem, and defines a certain model to approximate the original objective function around the current best solution. Then, it takes a forward step based on the approximate model - find a solution as the next iteration point. The approximation model is only “trusted” in the neighborhood around the current iteration. The trust region is improved by iterations.

In this paper, one of the trust region methods - bound optimization by quadratic approximation (BOBYQA) method (Powell, 2009) is used to minimize the difference between observed first arrival times and simulated first arrival times. In the BOBYQA method, the trust region optimization algorithm is applied for bound-constrained nonlinear optimization and the objective function is treated as a black box. In this method, the derivative of the objective function is not needed, alternatively, at each iteration a local quadratic model $Q(X)$ of the objective function is built by multivariate interpolation in combination with trust region techniques. $g(X)$ is used to represent the objective function. The quadratic model has the form,

$$Q(X + d) = Q(X) + d^T \nabla Q(X) + \frac{1}{2} d^T \nabla^2 Q(X) d, \quad (1)$$

And Eq. (1) is solved by conditioning Eq. (2)

$$Q(X_i) = g(X_i), \quad \forall i \in \{1 \dots m\} \quad (2)$$

here n is the number of control variables and m is any number between $(n + 2)$ and $(2n + 1)$. In our problem, the quadratic model $Q(X)$ is built by $(m = n + 2)$ function evaluations. BOBYQA method uses the least Frobenius norm updating strategy, and we solve the following optimization problem at each iteration,

$$\min \quad \|\nabla^2 \varrho_t\|_F \quad (3)$$

$$\text{s.t.} \quad \varrho_t(X^+) = 1, \quad \varrho_t(X) = 0, \quad X \in \mathbf{X} \setminus X_t \quad (4)$$

where ϱ_t is a second order polynomial that needs to be determined, X is the current set of interpolation points, X^+ is a new point added to X and X_t is a point deleted from X (Powell, 2009). $\|A\|_F$ represents the Frobenius norm of matrix A , and for a $n \times n$ matrix A with

entries a_{ij} , $i, j \in \{1 \dots n\}$, the Frobenius norm is

$$\|A\|_F = \sqrt{\sum_{i,j=1}^n a_{ij}^2} \quad (5)$$

Then, the new model $Q^+(X)$ is updated by

$$Q^+(X) = Q(X) + \{g(X^+) - Q(X^+)\}_{\ell_t(X)} \quad (6)$$

where $\ell_t(X)$ is the solution of Eq. (3) which can be computed by solving a linear system (Powell, 2009).

Trust region method could guarantee to build the quadratic model with the global convergence and the good local sampling. Moré and Wild (2009) shows in their paper that this trust region method performs better than other optimization methods without explicit gradient computations. For the problem with less than a hundred unknowns, BOBYQA is expected to converge faster because it extracts local second order Hessian information. In this paper, trust region method is used to estimate the water-air contact and initial water saturation using seismic first arrival times.

4. Sand tank experiment

Sand tank experiment was being conducted at the wave tank facility (Coastal Studies Institute of Louisiana State University). The tank measures approximately $9 \times 6 \times 0.6$ m and contains a slightly heterogeneous sand pack that acts as a reservoir.

The sand tank is filled with water to a certain depth and configured with five wells to mimic reservoir production (Fig. 2). It provides production rate, bottom hole pressure and seismic first arrival times which will be integrated using the history matching method. This experiment is mainly used to test different history matching scenarios. In this paper, we are focusing on the integration of seismic first arrival times to improve the initial reservoir models. Two groups of seismic data were collected. The first one was collected at dry tank condition, and the second one was collected at the wet tank condition. For the wet tank condition, we filled the tank with water to 30.5 m depth, and waited for 15 h until the water almost fully penetrated the sand tank and the water levels in all the wells were stabilized and the same. Fig. 3 shows a 20 kHz seismic source and 8 accelerometers which are used to collect seismic data, and the data was saved in the computer next to

the tank.

4.1. Experiment results

Fig. 4 shows the seismic data collected in both dry and wet conditions. Fig. 4(a) and (b) are the same data which collected at dry tank condition, and Fig. 4(c) and (d) are the same data which collected at the wet tank condition.

As we can see in Fig. 4(a) and (b) there appears to be two separate refractive layers, and a possible third layers interpreted using reflected arrivals in the sand tank. In Fig. 4(b) the first layer arrivals are indicated in red, the second layer in green. The reflections from the bottom of the tank in purple, and the surface waves in yellow.

In Fig. 4(c) and (d), there appears to be two separate refractive layers, and a possible third and fourth layers interpreted using reflected arrivals in the sand tank. In Fig. 4(d) the first layer arrivals are indicated in red, the second layer in green. The reflections from the capillary fringe are indicated in blue, the reflections from the bottom of the tank in purple, and the surface waves in yellow.

The seismic first arrival times are picked, because based on the design of this experiment they are integrated to improve the flow models. In Fig. 5, the seismic first arrival times are selected from raw seismic data (Fig. 4). For the wet tank, the first arrival times are obtained at initial conditions (before the wells produced water). The first arrival times of the dry tank are different from the ones of wet tank, because there is no water in the dry tank and the seismic velocities are different from the ones in the wet tank.

5. Integration of seismic first arrival times

To integrate seismic first arrival times, both the synthetic, computed first arrival time and the observed first arrival times are needed. The synthetic and computed first arrival times are obtained by raytracing - simulation of seismic wave propagation, which depends on the medium velocities, and the observed first arrival times are picked from the seismic data.

In our work, the velocity models are computed by the Gassmann, Biot and Hertz-Mindlin method (Bachrach, Dvorkin, and Nur, 1998b; Appendix A), and the raytracing results are obtained through running FAST (Zelt and Ellis, 1988), a 2-D seismic tomography program. In Zelt's method, the velocity model is described as a series of trapezoidal blocks with vertical sides and upper and



Fig. 2. Sand tank experiment site with five wells, seismic source and accelerometers.



Fig. 3. Seismic source and accelerometers.

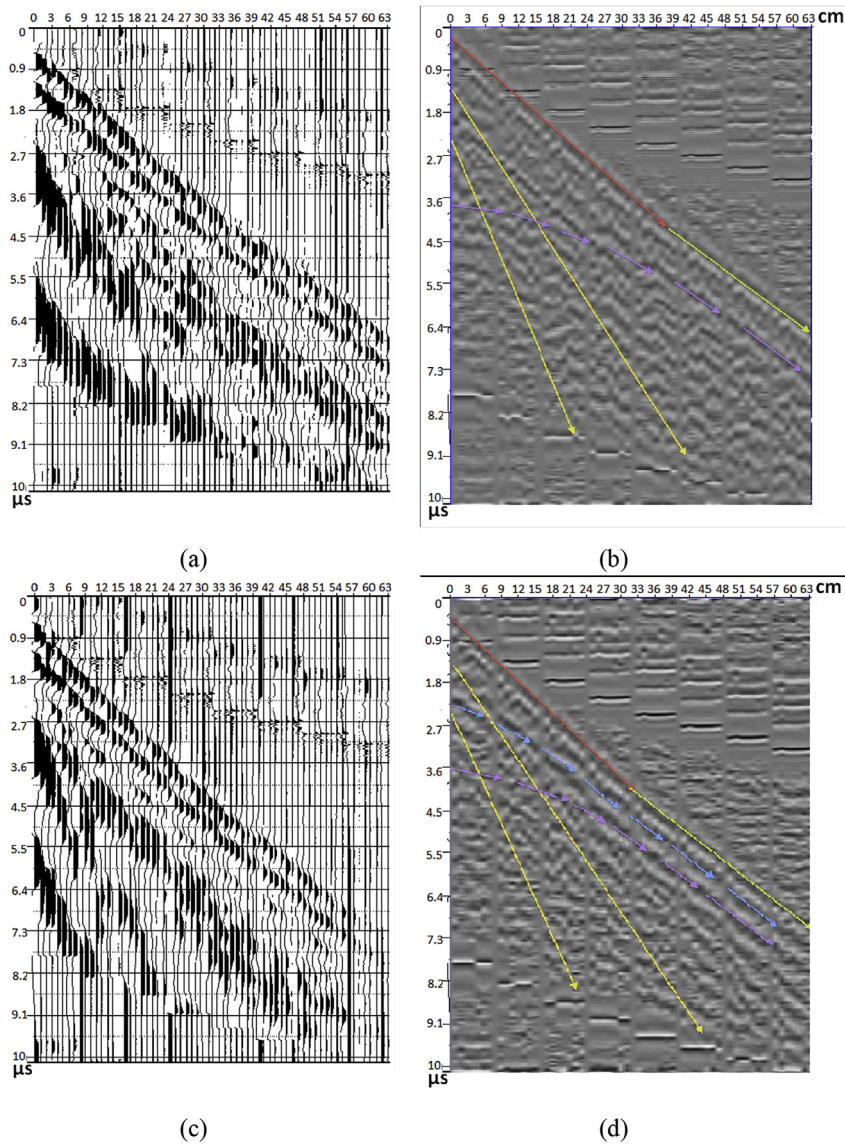


Fig. 4. The figures on the left are the wiggle plots and figures on the right are the image plots. (a) and (b) are the seismic plots of dry tank with no water added, and (c) and (d) are the seismic plots of sand tank filled with water. The surface waves and some noise from collection equipments are clearly presented (Chollett, 2012).

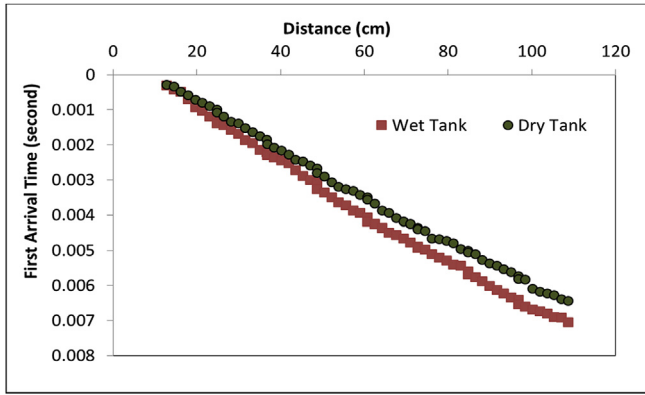


Fig. 5. First arrival times selected from raw seismic data. Seismic source is located at original point. The green circles show the first arrival times for the dry tank case. For the wet tank, the red squares shows the first arrival time obtained at initial conditions. (For interpretation of the references to colour in this figure legend, the reader is referred to the web version of this article.)

lower boundaries of arbitrary dip. Within each layer, the compressional wave velocity structure is defined by specifying a single upper and lower layer velocity for each trapezoidal block. To trace rays through the velocity model, the ray tracing equations are solved numerically (Cerveny et al., 1977; McMechan and Mooney, 1980). The two-dimensional ray tracing equations solved are a pair of first order ordinary differential equations in two sets:

$$\frac{dz}{dx} = \cot\theta \tag{7}$$

$$\frac{d\theta}{dx} = \frac{v_z - v_x \cot\theta}{v} \tag{8}$$

Where the variable θ is the angle between the tangent to the ray and the z axis, v is the velocity, and v_x and v_z are partial derivatives of velocity with respect to x and z (Zelt and Ellis, 1988). To solve either system, the routine uses the Runge Kutta method (Sheriff and Geldart, 1983) with error control suggested by Cerveny et al. (1977).

The observed first arrival times are picked from the seismic data of the experiment by a first arrival auto-picking program in Seismic Unix. Trust region method is used here to minimize the differences between the computed and observed first arrival time, and in this process, the initial water saturation, water-air contact, Poisson's ratio and coordination number are adjusted, and meanwhile the other parameters are considered as constants (Table 1).

Since the seismic first arrival times from both dry tank and wet tank are collected, and water-air contact and initial water saturation do not impact the seismic first arrival times of dry tank, we consider to integrate seismic first arrival times separately. The ones from dry tank are integrated first to estimate the coordination

Table 1
The values of the other parameters used to calculate velocities.

Quantity	Symbol	Value	Units
Bulk modulus of water	K_{water}	2.2×10^9	Pa
Bulk modulus of air	K_{air}	1.01×10^5	Pa
Mineral bulk modulus	K_0	36.6×10^9	Pa
Framework dry shear modulus	G_{dry}	45.0×10^9	Pa
Water density	ρ_{water}	1000	kg/m ³
Air density	ρ_{air}	0.18	kg/m ³
Mineral density	ρ_{quartz}	2650	kg/m ³

number and Poisson's ratio, and then the ones from wet tank are integrated to estimate the water-air contact and initial water saturation.

For the dry tank, only the coordination number and Poisson's ratio are estimated. The trust region method is used here, and after 7 iterations (raytracing runs), the best match of simulated and observed first arrival times is obtained with coordination number and Poisson's ratio to be 4.6 and 0.253 (Fig. 6). This result proves that the velocity of sand tank calculated by Hertz-Mindlin theory and Gassmann equation (Appendix A) is reasonable, and it can be used to simulate the wave propagations in the sand tank. In Fig. 6, what needs to explain is that the lower part of first arrival times has a better match than the upper part, this is because the coordination numbers are assumed to be the same everywhere in sand tank. If different coordination numbers are used between layers, a better match could be obtained.

For the wet tank, if we assume that the tank was fully saturated below the water table (initial water saturation equals one), the simulated first arrival times are much earlier than the observed ones at the receivers more than 40 cm away from seismic source (Fig. 7). It was caused by the calculated high velocity zone below

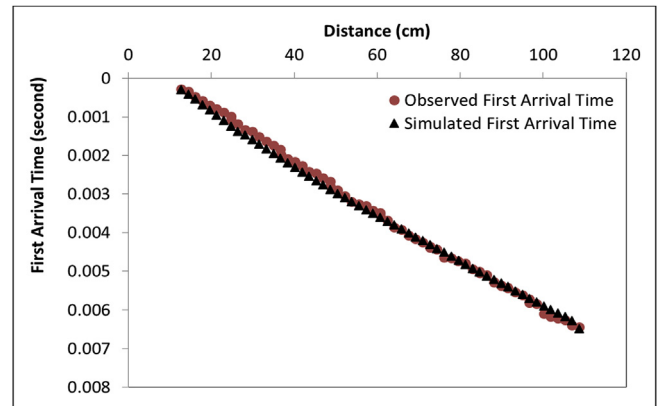


Fig. 6. Simulated seismic first arrival time of the dry tank. The x-axis is the receiver position in centimeter and y-axis is first arrival time in second. The red circles show the observed first arrival time and the black triangles show the best match of simulated first arrival time. (For interpretation of the references to colour in this figure legend, the reader is referred to the web version of this article.)

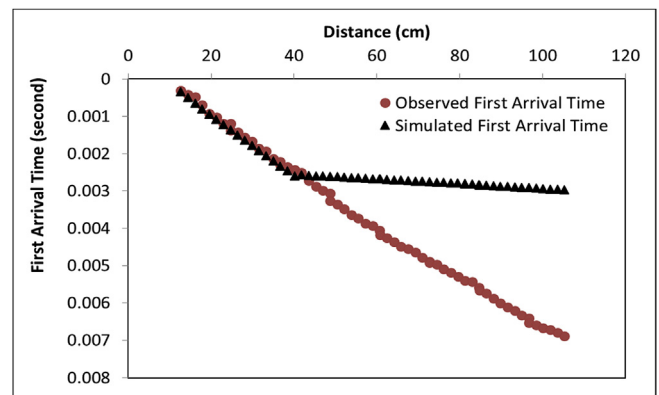


Fig. 7. Simulated seismic first arrival times (triangles) of the wet tank calculated using 100% initial water saturation. The red circles show the observed first arrival times and the black triangles show the simulated first arrival time. The simulated first arrival times are matched for the receivers near the source (less than 40 cm), but are very different for the receivers far away from the source (more than 40 cm). (For interpretation of the references to colour in this figure legend, the reader is referred to the web version of this article.)

the water table since the velocity increases dramatically near the fully saturated point (Fig. 3).

Since the coordination number and Poisson's ratio are obtained through the integration of dry tank first arrival times, to match the first arrival times in wet tank, only the water-air contact and initial water saturation are unknown and are adjusted. After 8 raytracing iterations using trust region method, the best match of simulated

and observed first arrival times is obtained with water-air contact and initial water saturation to be 18.7 cm deep and 0.78 (Fig. 8). The calculated water-air contact depth is very close to the depth we measured at the production well – 19.2 cm. For the wet tank results, the upper and lower parts are not matched very well since a single coordination number is used here for the whole model, and this could be improved by using several coordination numbers for different layers.

Forty sand tank simulation models are generated by using unconditional gaussian simulation, and they have different permeability and porosity distributions. Fig. 9 shows that the predicted production rates of these forty models and the water table levels in these models are different. Figure shows the predicted production rates of the sand tank models with water table level updated based on matching results of seismic first arrival times. Compared the predictions in Figs. 9 and 10, we can clearly conclude that the first arrival times have help improve the models, and the uncertainty of models have been decreased dramatically.

6. Conclusions

In this paper, a methodology and motivation for integrating the first arrival seismic data without an inversion step has been introduced, and the seismic data of sand tank experiment is used to test it. The trust region method is used as integration method, and the result shows that the estimation of water-air contact and initial water saturation in the sand tank is improved by integrating

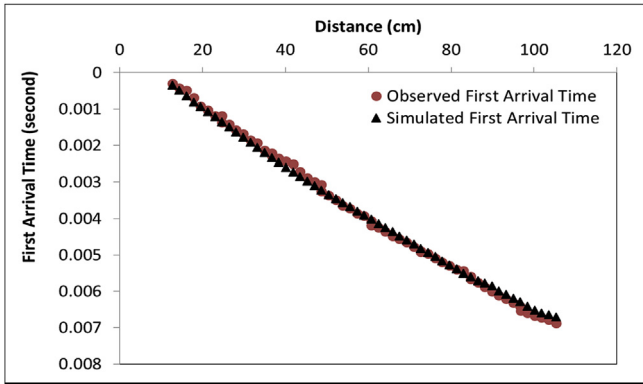


Fig. 8. Best match of simulated first arrival time of the wet tank. The initial water saturation is 0.78 saturation. The red circles show the observed first arrival time and the black triangles show the simulated first arrival time. The simulated and observed first arrival time is matched well. (For interpretation of the references to colour in this figure legend, the reader is referred to the web version of this article.)

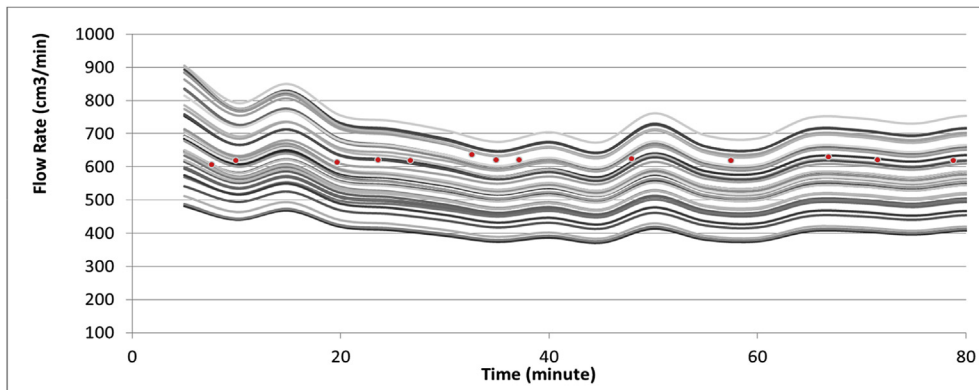


Fig. 9. The predicted production rates for the sand tank models. The grey curves indicate the simulations of forty models and the red points indicate the measured flow rate. (For interpretation of the references to colour in this figure legend, the reader is referred to the web version of this article.)

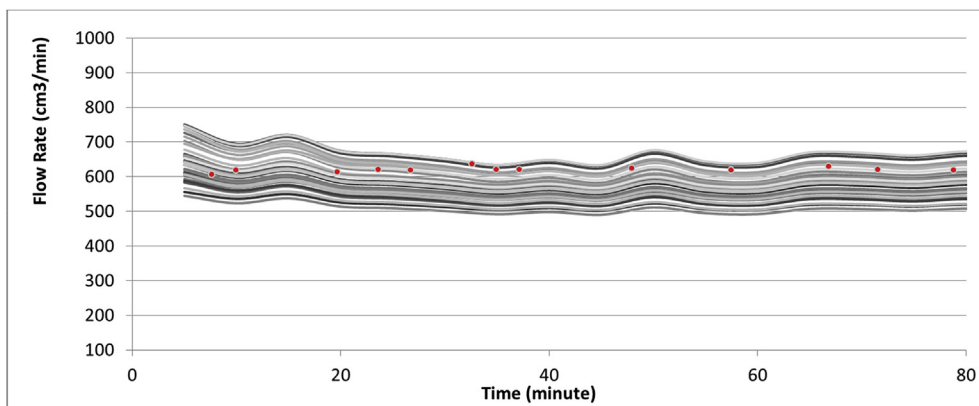


Fig. 10. The predicted production rates of the sand tank models with water table level updated. The grey curves indicate the simulations of forty models and the red points indicate the measured flow rate. (For interpretation of the references to colour in this figure legend, the reader is referred to the web version of this article.)

seismic first arrival times. Several contributions could be summarized as below:

1. A new method of using the seismic data to improve the fluid models has been introduced, though we only use the first arrival times of seismic data. Compared to the previous methods, the new method integrates the seismic data directly by comparing with raytracing results instead of inverting seismic data to seismic impedance values first, which are also nonunique (Saltzer and Finn, 2006).
2. The uncertainty of velocity models has been taken into consideration in the process of integrating seismic data. Since when we run the raytracing to simulate seismic first arrival times, the parameters that affect velocity models are adjusted, such as coordination number, Poisson's ratio, water-air contact and initial water saturation, while in the integration of seismic impedance data the velocity model is assumed known.
3. Trust region method is used as integration method in this paper. It works very efficiently and the best matching results are obtained in a few simulation runs. The limitation of trust region method is that the number of simulation runs is related with the number of tuning parameters, if there are more tuning parameters, such as porosity, permeability and pressure in the fluid model, the number of simulation runs increases dramatically, in this case the methods such as ensemble Kalman filter are a better choice.
4. In this paper, the sand tank experiment data has been used to test the new method, and it has been proved that Biot and Gassmann equation could be used to estimate the velocity profile of sand tank experiment.
5. The comparison in Figs. 9 and 10 shows that the prediction of simulation models have been improved dramatically with the water level updated by matching first arrival times. This could be applied in oil industry to estimate the water-oil contact by setting up seismic source and received along the well bore.

Acknowledgements

This work was done while the author was a PhD candidate at Louisiana State University. We acknowledge Shell E&P Technology Company for their monetary support for this project.

Appendix A

Elastic wave velocity can be calculated by Gassmann equation (Gassmann, 1951):

$$V_p = \sqrt{\frac{\bar{K} + \frac{4}{3}\bar{G}}{\bar{\rho}}}$$

$$V_s = \sqrt{\frac{\bar{G}}{\bar{\rho}}}$$

where V_p is the compressional wave, V_s is the shear wave, \bar{K} and \bar{G} are the effective material bulk and shear moduli respectively, and $\bar{\rho}$ is its bulk density.

At its low-frequency limit, \bar{K} and \bar{G} are calculated by Biot's theory (Biot, 1956a; 1956b):

$$\frac{K_{sat}}{K_0 - K_{sat}} = \frac{K_{dry}}{K_0 - K_{dry}} + \frac{K_{fl}}{\phi(K_0 - K_{fl})}$$

$$G_{sat} = G_{dry}$$

in which G_{dry} and K_{dry} are the dry framework shear and bulk moduli, respectively, K_0 is the mineral bulk modulus, K_{fl} is the pore fluid bulk modulus, and G_{sat} and K_{sat} are the saturated effective bulk moduli, respectively.

For rocks packed with water and air, K_{fl} is the harmonic average of the air bulk modulus K_{air} and the water bulk modulus K_{water} (Bachrach, Dvorkin, and Nur, 1998b),

$$\frac{1}{K_{fl}} = \frac{S_w}{K_{water}} + \frac{1 - S_w}{K_{air}}$$

G_{dry} and K_{dry} are calculated by the Hertz-Mindlin method (Bachrach, Dvorkin, and Nur, 1998a). It gives the relationships between the effective bulk and shear moduli for a dry, dense, random pack of identical spherical grains subject to effective stress, and includes the effect of coordination number, and the radius of contact.

$$K_{dry} = \left[\frac{z^2(1-\phi)^2 G^2}{18\pi^2(1-\nu)^2 p_{eff}} \right]^{\frac{1}{3}}$$

$$G_{dry} = \frac{5-4\nu}{5(2-\nu)} \left[\frac{3z^2(1-\phi)^2 G^2}{2\pi^2(1-\nu)^2 p_{eff}} \right]^{\frac{1}{3}}$$

where z is the coordination number, ϕ is the porosity, G is the shear modulus of grains, ν is Poisson's ratio and p_{eff} is the effective stress.

References

- Bachrach, Ran, Dvorkin, Jack, Nur, Amos, 1998a. High-resolution shallow seismic experiments in sand, part II: velocities in shallow unconsolidated sand. *Geophysics* 63 (4), 1234–1240 (July–August).
- Bachrach, Ran, Dvorkin, Jack, Nur, Amos, 1998b. High-resolution shallow-seismic experiments in sand, part I: water table, fluid flow and saturation. *Geophysics* 63 (4), 1225–1233 (July–August).
- Biot, M.A., 1956a. Theory of propagation of elastic waves in fluid-saturated porous solid. I. Higher-frequency range. *J. Acoust. Soc. Am.* 28 (2), 179–191 (March).
- Biot, M.A., 1956b. Theory of propagation of elastic waves in fluid saturated porous solid. II. Low-frequency range. *J. Acoust. Soc. Am.* 28 (2), 168–178 (March).
- Cerveny, V., Molotkov, I., Psencik, I., 1977. *Ray method in Seismology*. Charles University Press.
- Chollett, Shannon, 2012. *An Experimental and Theoretical Critique of Flow Model Accuracy*. Master's thesis. Louisiana State University.
- Dong, Yannong, 2005. *Integration of Time-lapse Seismic Data into Automatic History Matching*. Ph.D. diss. The University of Oklahoma.
- Emerick Alexandre Anozé, Rafael Jesus de Moraes, and José Roberto Pereira Rodrigues. 2007, June. "History Matching 4D Seismic Data With Efficient Gradient-Based Methods." EUROPEC/EAGE Conference and Exhibition. London, U.K. SPE-107179-MS.
- Gassmann, Fritz, 1951. Elastic waves through a packing of spheres. *Geophysics* 16 (4), 673–685 (May).
- Li Gaoming, Mei Han, R. Banerjee, and A.C. Reynolds. 2009, October. "Integration of Well Test Pressure Data Into Heterogeneous Geological Reservoir Models." SPE Annual Technical Conference and Exhibition. New Orleans, Louisiana. SPE-124055-MS.
- McMechan, G.A., Mooney, W.D., 1980. Asymptotic ray theory and synthetic seismograms for laterally varying structures: theory and application to Imperial Valley, California. *Bull. Seism. Soc. Am.* 70, 2021–2035.
- Moré, Jorge J., Wild, Stefan M., 2009. Benchmarking derivative-free optimization benchmarking derivative-free optimization algorithms. *SIAM J. Optim.* 20 (1), 172–191.
- Powell, M.J.D., 2009. *The BOBYQA Algorithm for Bound Constrained Optimization without Derivatives*. Report DAMTP 2009/NA06. Centre for Mathematical Sciences, University of Cambridge, UK.
- Saltzer Rebecca, and Chris Finn. 2006. "Exploiting the non-uniqueness of seismic inversion to obtain alternate scenarios of economic interest." SEG/New Orleans Annual Meeting.
- Sheriff, R.E., Geldart, L.P., 1983. *Exploration Seismology, Volume 2: Data Processing and Interpretation*. Cambridge University Press.

- Skjervheim, J.A., Evensen, G., Aanonsen, S.I., Ruud, B.O., Johansen, T.A., 2007. Incorporating 4D seismic data reservoir simulation models using ensemble Kalman filter. *SPE J.* 12 (3), 282–292. SPE-95789-PA.
- Thulin Kristian, Gaoming Li, Sigurdvar Aanonsen, and Albert C. Reynolds. 2007, November. "Estimation of Initial Fluid Contacts by Assimilation of Production Data With EnKF." SPE Annual Technical Conference and Exhibition, Anaheim, California. SPE-109975-MS.
- Valestrand, Randi, Sagen, Jan, Nævdal, Geir, Huseby, Olaf, 2010. The effect of including tracer data in the ensemble-kalman-filter approach. *SPE J.* 15 (2), 454–470. SPE-113440-PA.
- Zelt, C.A., Ellis, R.M., 1988, June. Practical and Efficient Ray Tracing in Two-dimensional Media for Rapid Traveltime and Amplitude Forward Modeling.
- Zhao, Yong, Reynolds, Albert C., Li, Gaoming, 2008. Generating Facies Maps by Assimilating Production Data and Seismic Data with the Ensemble Kalman Filter. SPE/DOE Symposium on Improved Oil Recovery. Tulsa, Oklahoma. SPE-113990-MS.